BEAM DYNAMICS CALCULATIONS FOR ALVAREZ-TYPE LINEAR ACCELERATORS*

Marvin Rich
Los Alamos Scientific Laboratory, University of California
Los Alamos, New Mexico

I. Introduction

Detailed beam dynamics studies for Alvarez-type linear accelerators have generally been done on high speed computers using impulse-type approximations to simulate the particle acceleration within a gap or direct numerical integrations of the equations of motion. In this summary we would like to describe a procedure for studying such beam dynamics which retains most of the accuracy of the numerical integration without an excessive loss of computational speed as compared to the impulse approximation method. In addition, the results of some calculations for the proposed LASL meson factory will be presented.

Briefly, the procedure which has been used consists of assuming that the axial electric field within a gap between drift tubes is spatially constant and zero within the drift tubes. (A more general axial field could be used but with added complications.) This is as opposed to the more usual procedure of using the principal harmonic of the axial field within the gap. Using Maxwell's equations and the axial field form, the off-axis electric and magnetic fields can be obtained as a power series in the radial coordinate, r. This has been done through terms in r^3. In addition, one obtains radial and longitudinal impulsive terms which a particle will experience on entering or leaving a gap. Using the electromagnetic fields obtained in this way, an approximate solution to the relativistic equations of motion for a particle within a gap has been constructed. The impulses at the extremities of the gap are, of course, easily treated.

Comparisons of accelerator calculations using the approximate solutions mentioned above and an accurate numerical integration of the particle equations of motion have been made. Agreement to about four significant figures in energy and phase (absolute phase, not phase relative to the accelerator design particle) was found after passage of particles through 250 gaps. Similar comparisons using an impulse approximation treatment with the same accelerator design were noticeably poorer, particularly with respect to the final phase.

*Work performed under the auspices of the U. S. Atomic Energy Commission.

II. Method of Calculation

Only an outline of the computational procedure will be given. This may be divided into three parts:

(a) the form for the electromagnetic fields within a gap;
(b) the approximate solution of the particle equations of motion;
(c) the beam dynamics code.

A. The Gap Fields

For the purpose of the calculation it is assumed that the z-component of the electric field has the following spatial form on the axis, r = 0:

$$\begin{aligned} E_z(0,z) &= 0 && -L/2 \le z < -g/2 \\ &= E_0 f(z) && -g/2 \le z \le g/2 \\ &= 0 && g/2 < z \le L/2 \end{aligned} \qquad (1)$$

where L is the distance between drift tube centers as illustrated in Fig. 1 and g is the gap length. The field may be thought of as periodic with period L and its time dependence is taken as cos ωt.

Using the knowledge of the E_z field at r = 0 and Maxwell's equations, the off-axis fields in the gap may be obtained as a power series in r, the first few terms of which give

$$\left.\begin{aligned} E_z(r,z,t) &= E_0 F(r,z) \cos \omega t \\ E_r(r,z,t) &= -E_0 G(r,z) \cos \omega t \\ B_\theta(r,z,t) &= -E_0 Q(r,z) \sin \omega t \end{aligned}\right\} \quad -g/2 \le z \le g/2 \qquad (2)$$

where

$$\begin{aligned} F(r,z) &= f(z) + \frac{1}{4} r^2 S(z) \\ G(r,z) &= \frac{1}{2} r \left[\delta(z + g/2) f(z) - \delta(z - g/2) f(z) + \frac{df}{dz}\right] \\ &\quad + \frac{1}{16} r^3 \frac{dS(z)}{dz} \\ Q(r,z) &= \frac{1}{2} r \frac{\omega}{c^2} f(z) + \frac{1}{16} r^3 \frac{\omega}{c^2} S(z) \end{aligned} \qquad (3)$$

and

$$S(z) = -\frac{\omega^2}{c^2} f(z) - \frac{d}{dz}\left[\delta(z + g/2) f(z) - \delta(z - g/2) f(z)\right] .$$

If the δ-functions are treated as slightly smeared δ-functions, representing the fall off of the fields within the drift tube hole, and it is assumed that a particle does not change its position or velocity appreciably over the fall-off region, then these terms merely contribute an impulse to a particle on entering and leaving a gap. The approximate effect of this impulse is given below in Eq. (7). Neglecting the impulse producing terms, the fields within a gap are

$$\left.\begin{aligned} E_z &= E_0 f(z)\left[1 - \frac{1}{4}\frac{\omega^2}{c^2} r^2\right] \cos \omega t \\ E_r &= -E_0 \frac{df(z)}{dz}\left[\frac{1}{2} r - \frac{1}{16}\frac{\omega^2}{c^2} r^3\right] \cos \omega t \\ B_\theta &= -E_0 \frac{\omega}{c^2} f(z)\left[\frac{1}{2} r - \frac{1}{16}\frac{\omega^2}{c^2} r^3\right] \sin \omega t \end{aligned}\right\} \quad -g/2 < z < g/2 . \quad (4)$$

In the following, $f(z)$ has been taken equal to unity, giving $E_r = 0$ within the gap.

B. Approximate Solution of the Equations of Motion

In Cartesian coordinates, the relativistic equations of motion for a particle moving in an electromagnetic field of the sort given in Eq. (3) are

$$\left.\begin{aligned} \frac{du_1}{dt} &= \frac{e}{m}\left[E_r - v_3 B_\theta\right]\frac{x_1}{r} \\ \frac{du_2}{dr} &= \frac{e}{m}\left[E_r - v_3 B_\theta\right]\frac{x_2}{r} \\ \frac{du_3}{dt} &= \frac{e}{m}\left[E_z + (v_1 x_1 + v_2 x_2) B_\theta / r\right] \end{aligned}\right\} \quad (5)$$

$$\frac{dx_i}{dt} = u_i/\gamma = v_i \qquad i = 1, 2, 3 \quad (6)$$

where indices 1, 2, and 3 correspond to the x, y, and z directions, respectively, $r = \sqrt{x_1^2 + x_2^2}$, and $\gamma = \sqrt{1 + \vec{u}^2/c^2}$. From Eqs. (2), (3), and (5) it can be shown that the change in u_i due to the impulse occurring on entering a gap is approximately

$$\Delta u_1 = -\frac{e}{m} E_0 f(-g/2) x_1 \left(\frac{1}{2} - \frac{1}{16}\frac{\omega^2}{u_3^2} r^2\right)\frac{\gamma}{u_3} \cos \omega t$$

$$\Delta u_2 = -\frac{e}{m} E_0 f(-g/2) x_2 \left(\frac{1}{2} - \frac{1}{16}\frac{\omega^2}{u_3^2} r^2\right)\frac{\gamma}{u_3} \cos \omega t \qquad (7)$$

$$\Delta u_3 = -\frac{e}{m} E_0 f(-g/2)\frac{\gamma}{u_3}\left(\frac{1}{4} r^2 \omega \gamma / u_3 \sin \omega t + \frac{1}{16}\frac{\omega^2}{c^2} r^2 \frac{u_1 x_1 + u_2 x_2}{u_3} \cos \omega t\right)$$

where the coordinates, u components, and time are those corresponding to the arrival at the gap. Similar equations with opposite signs apply on leaving the gap.

A relatively accurate approximate solution of the equations of motion across the gap can be obtained by assuming that the components of velocity may be written in the form

$$v_i(t) = v_0^{(i)} + v_1^{(i)} t + f^{(i)}\left[\cos(\omega t + \psi_0) - \cos \psi_0\right] + g^{(i)}\left[\sin(\omega t + \psi_0) - \sin \psi_0\right] \qquad (8)$$

where ψ_0 is the phase of the cavity field when the particle enters the gap and the z-coordinate and time at the beginning of the gap are taken as $z = 0$ and $t = 0$. Equation (8) is actually part of a more general ansatz that can be made for the velocity. The coordinates are then approximately

$$x_i(t) = x_0^{(i)} + \left[v_0^{(i)} - f^{(i)} \cos \psi_0 - g^{(i)} \sin \psi_0\right] t + \frac{1}{\omega} f^{(i)}\left[\sin(\omega t + \psi_0) - \sin \psi_0\right] - \frac{1}{\omega} g^{(i)}\left[\cos(\omega t + \psi_0) - \cos \psi_0\right]. \qquad (9)$$

If the coordinates and velocities given in Eqs. (8) and (9) are inserted into Eq. (5) for the u_i, using the previously described fields with $f(z) = 1$, the u_i can be obtained upon integration. These values of u_i and the relation $v_i = u_i/\sqrt{1 + \vec{u}^2/c^2}$ may then be used to identify the coefficients $v_1^{(i)}$, $f^{(i)}$, and $g^{(i)}$. When small terms are neglected, one obtains

$$
\begin{aligned}
v_1^{(i)} &= \left[u_1^{(i)} - v_0^{(i)} \vec{v}_0 \cdot \vec{u}_1 / c^2 \right] / \gamma_0 \qquad i = 1, 2, 3 \\
f^{(1,2)} &= a^{(1,2)} / \gamma_0 \\
f^{(3)} &= - v_0^{(3)} \vec{v}_0 \cdot \vec{a} / (\gamma_0 c^2) \\
g^{(1,2)} &= - v_0^{(1,2)} \vec{v}_0 \cdot \vec{b} / (\gamma_0 c^2) \\
g^{(3)} &= b^{(3)} / \gamma_0 - v_0^{(3)} \vec{v}_0 \cdot \vec{b} / (\gamma_0 c^2)
\end{aligned}
\tag{10}
$$

where

$$\gamma_0 = 1 / \sqrt{1 - \vec{v}_0^{\,2} / c^2} \quad , \quad \text{and}$$

$$u_1^{(i)} = - \frac{e}{m} E_0 \frac{\cos \omega_0}{c^2} \left\{ \left(\frac{1}{2} - \frac{1}{16} \frac{\omega^2}{c^2} r^2 \right) v_0^{(i)} - \frac{1}{8} v_0^{(3)} x_0^{(i)} \frac{\omega^2}{c^2} \sum_{k=1}^{2} x_0^{(k)} v_0^{(k)} \right\}$$

$$a^{(i)} = - \frac{e}{m} E_0 \frac{v_0^{(2)}}{c^2} x_0^{(i)} \left(\frac{1}{2} - \frac{1}{16} \frac{\omega^2}{c^2} r_0^2 \right) \qquad i = 1, 2$$

$$b^{(i)} = \frac{e}{m} E_0 \frac{v_0^{(3)}}{\omega c^2} v_0^{(i)} \left(\frac{1}{2} - \frac{1}{16} \frac{\omega^2}{c^2} r_0^2 \right)$$

$$u_1^{(3)} = - \frac{e}{m} E_0 \frac{\sin \psi_0}{c^2} \left\{ \frac{\omega}{2} \sum_{k=1}^{2} x_0^{(k)} v_0^{(k)} - \left(\frac{1}{2} - \frac{1}{16} \frac{\omega^2}{c^2} r_0^2 \right) \sum_{k=1}^{2} v_0^{(k)2} \right\} \tag{11}$$

$$a^{(3)} = 0$$

$$b^{(3)} = \frac{e}{m} E_0 \frac{1}{\omega} \left(1 - \frac{1}{4} \frac{\omega^2}{c^2} r_0^2 \right) .$$

In the limit of pure phase motion one has

$$u_3 = u_0^{(3)} + \frac{e}{m} E_0 \frac{1}{\omega} \left[\sin (\omega t + \psi_0) - \sin \psi_0 \right]$$

$$v_3 = v_0^{(3)} + \frac{e}{m} E_0 \frac{1}{\omega \gamma_0^3} \left[\sin (\omega t + \psi_0) - \sin \psi_0 \right] \tag{12}$$

$$x_3 = x_0^{(3)} + \left[v_0^{(3)} - \frac{e}{m} E_0 \frac{1}{\omega \gamma_0^3} \sin \psi_0 \right] t - \frac{e}{m} E_0 \frac{1}{\omega^2 \gamma_0^3} \left[\cos (\omega t + \psi_0) - \cos \psi_0 \right] .$$

C. The Beam Dynamics Code

The beam dynamics code which has been written using the above results is essentially the same as most such codes. However, the method for specification of the accelerator geometry is perhaps somewhat different from what is usual and should be described. Here, input values of stable phases and the g/L sequences for each tank are used to define an entering and an exiting phase of the "stable particle" in any gap, say gap n, by

$$\psi_{in}(n) = \psi_{stable} - \pi(g/L)_n$$

$$\psi_{out}(n) = \psi_{stable} + \pi(g/L)_n \quad .$$

Starting at the end of the $(n-1)^{th}$ gap with longitudinal velocity v_{n-1}, the length of the $(n-1)^{th}$ drift tube is taken as

$$d_{n-1} = (\psi_{in}(n) - \psi_{out}(n-1) + 2\pi) \cdot v_{n-1}/\omega \quad .$$

The length of the n^{th} gap and the velocity v_n at the end of this gap are obtained from Eq. (12), where the time to be used is $t = (\psi_{in}(n) - \psi_{out}(n))/\omega$ since the field was assumed to have phase $\psi_{in}(n)$ when the particle entered the gap and phase $\psi_{out}(n)$ when it left. If ϵ_0 is the energy gain per meter in the tank containing gap n, the constant E_0 appearing in Eq. (12) is

$$E_0(n) = 2\pi\epsilon_0 / \left[\sin\psi_{out}(n) - \sin\psi_{in}(n)\right] .$$

When the geometry of the accelerator has been determined, particles with varying initial energy, phase, and off-axis position and velocity can be carried through the structure using Eqs. (8) through (11). The time required to cross a gap is first obtained by iterating the $z \equiv x_3$-coordinate equation in the form

$$t_{k+1} = \left\{ g + \frac{f^{(3)}}{\omega}\left[\sin(\omega t_k + \psi_0) - \sin\psi_0\right] - \frac{g^{(3)}}{\omega}\left[\cos(\omega t_k + \psi_0) - \cos\psi_0\right]\right\} \times \left[v_0^{(3)} - f^{(3)}\cos\psi_0 - g^{(3)}\sin\psi_0\right]^{-1}$$

using an initial guess of $t_0 = (\psi_{in} - \psi_{out})/\omega$. It has been found that two to three iterations are required for four-digit convergence. With this time interval, the remaining particle parameters are found by substitution into the remaining equations. Transit through quadrupole

magnets in drift tube sections is accomplished by the standard linear approximation.

The code also contains provisions for studying random errors in tank phase, tank or gap field amplitudes, drift tube and quadrupole misalignment, and quadrupole field magnitude.

III. Some Preliminary Results

Very little has been done as yet with regard to radial motion studies using the code described above. However, fairly extensive phase motion calculations have been made on a number of accelerator designs. In these, phase-energy acceptance "fishes" have been obtained with and without various types and combinations of random alignment and field errors, and output phase and energy spreads have been examined. A few examples of these results are given below for a geometry corresponding to the present design of the LASL meson factory. A definite statement about the effect of random errors will not be made since error studies for this geometry with many different sets of random inputs have not been completed.

Figure 2 shows a comparison of the phase and energy oscillations for a sample particle, using a numerical integration of the equations of motion (upper graph) and using Eqs. (12) (lower graph). The oscillatory solid lines give the phase motion and the dotted lines the energy deviations with respect to the stable particle. In Fig. 3 the acceptance fish for the design in Table I is shown (solid line) along with that when a particular set of random errors, specified in Table II, are introduced (dashed line). The effects of certain type errors, as tank-to-tank phase or field amplitude errors, have been found to have a more drastic effect on the acceptance region than when they are present as gap-to-gap errors. The remaining figures show the maximum phase and energy oscillation amplitudes of particles leaving the machine as a function of input phase and energy with and without the errors of Table II.

TABLE I

Specifications of the Drift Tube Portion of the LASL Linear Accelerator

Tank Number	1	2	3	4	5
Initial Energy	0.75	10.75	60.35	102.0	141.5
Final Energy	10.75	60.35	102.0	141.5	176.5
Stable Phase	-26^{o}	-26^{o}	-26^{o}	-26^{o}	-26^{o}
Energy gain/meter (MeV/m)	1.11	1.65	1.42	1.28	1.16
g/L Range	.2-.3	.19-.33	.35-.42	.40-.44	.43-.46
Drift Space (meters)	0.305	0.610	0.610	0.610	

TABLE II

Maximum Field and Alignment Errors for the Sample Problem

Axial Drift Tube Displacement Error	$\pm$ 0.001 m
Field Error for Drift Tube Gaps	$\pm$ 2%
Tank Field Error	$\pm$ 2%
Tank Phase Error	$\pm 1^{o}$

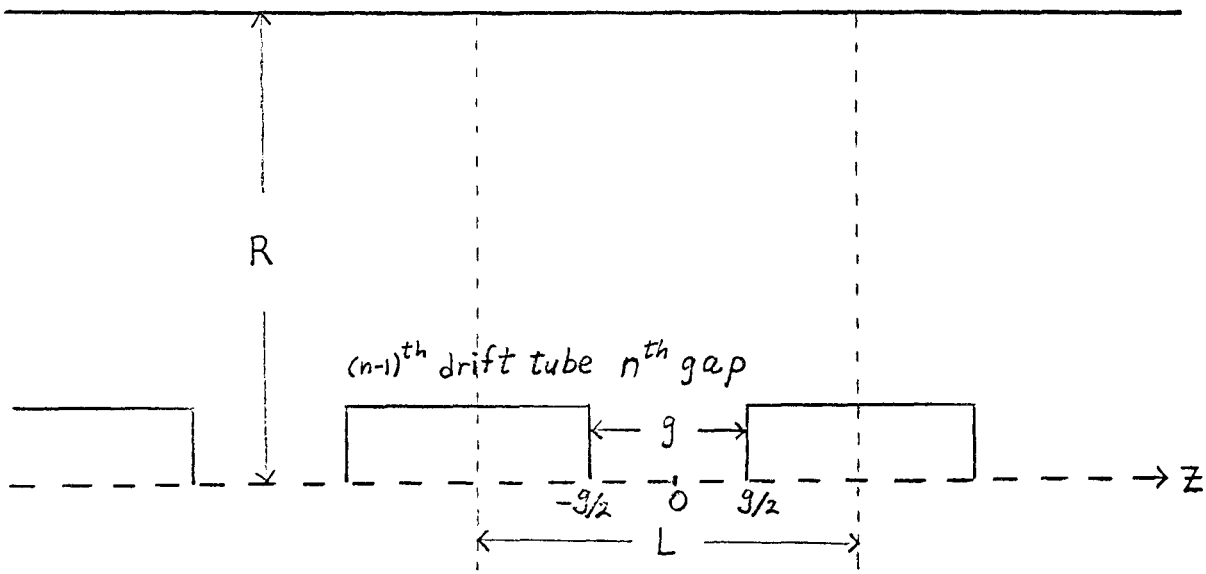

Figure 1: Schematic diagram of a drift tube section

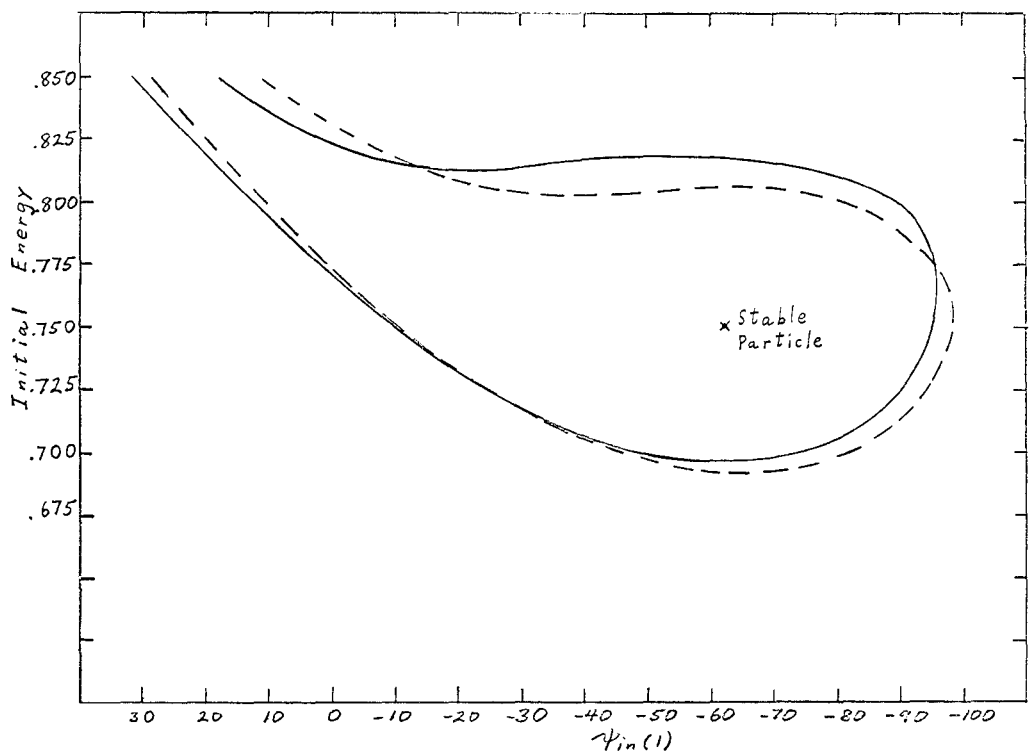

Figure 3: Phase-energy acceptance region for the accelerator geometry specified by Table I. The solid curve shows the acceptance when no errors are present and the dashed curve gives the acceptance for the errors of Table II.

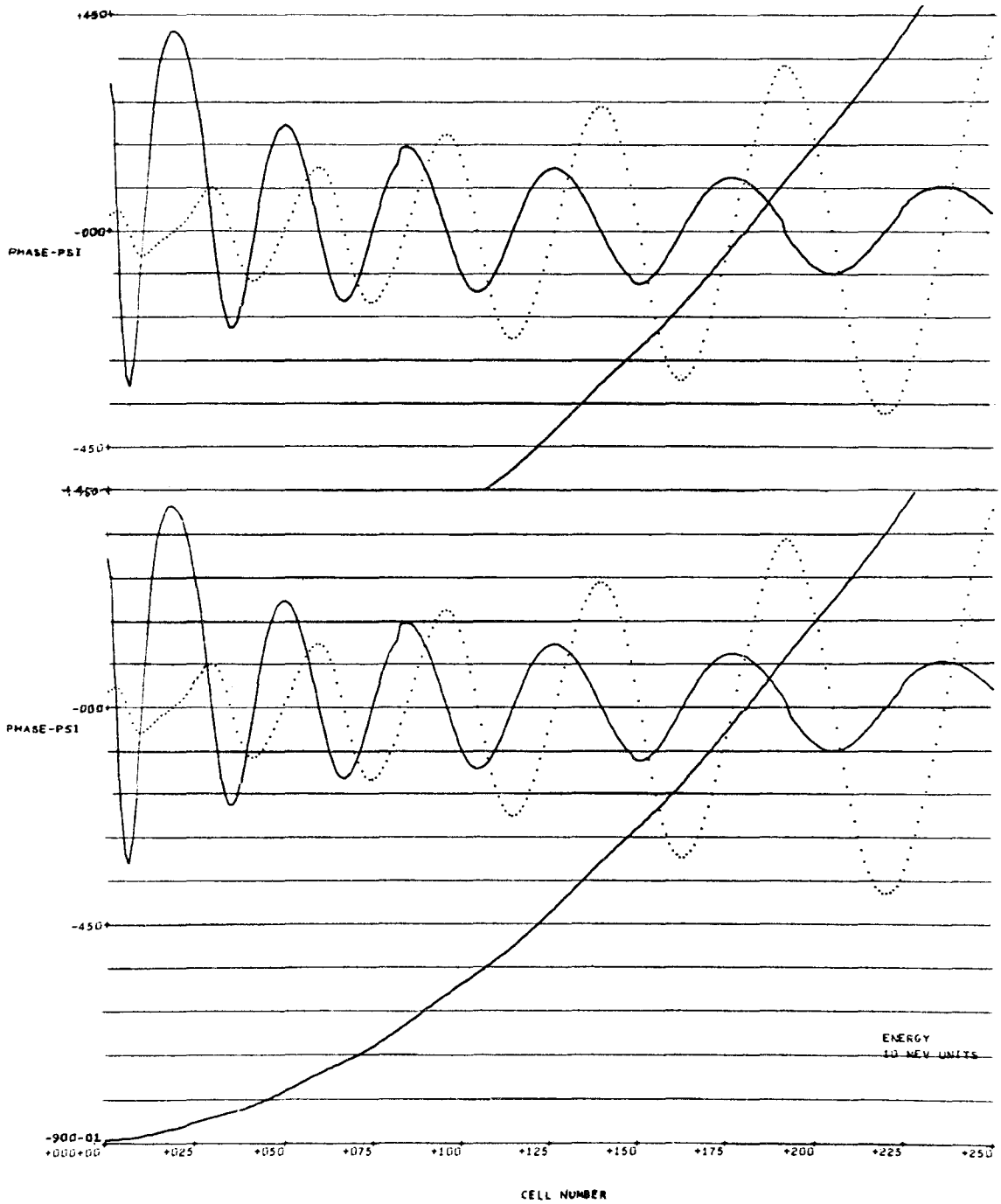

Figure 2: Comparison of phase and energy oscillations for a sample particle using a numerical integration of the particle equation of motion and using Equations (12).

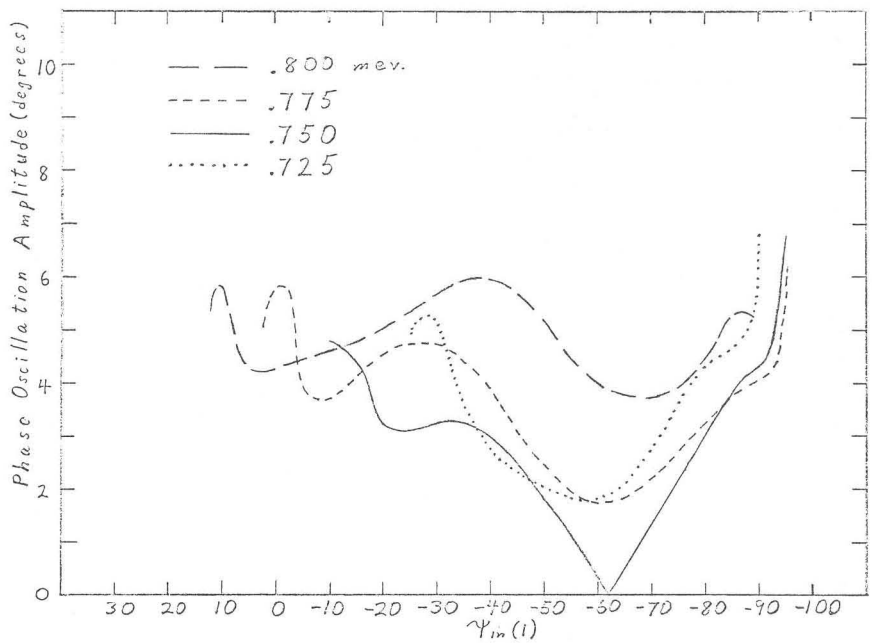

Figure 4: Final phase oscillation amplitude as a function of initial phase, $\psi_{in}(1)$, for various initial energies no errors are present.

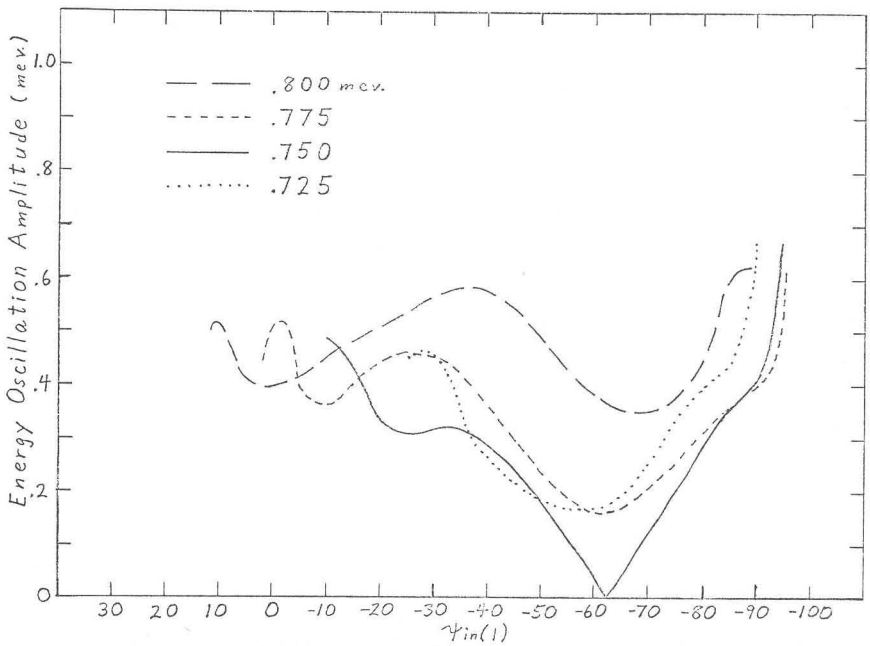

Figure 5: Final energy oscillation amplitude as a function of initial phase, $\psi_{in}(1)$, for various initial energies when no errors are present.

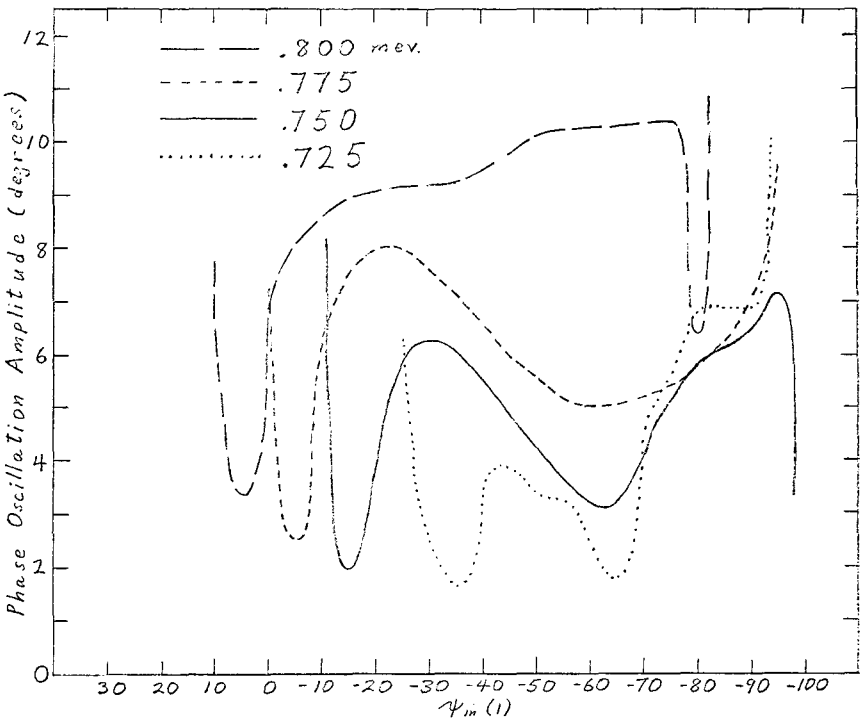

Figure 6: Final phase oscillation amplitude as a function of initial phase, $\psi_{in}(1)$, for various initial energies when the errors of Table II are present.

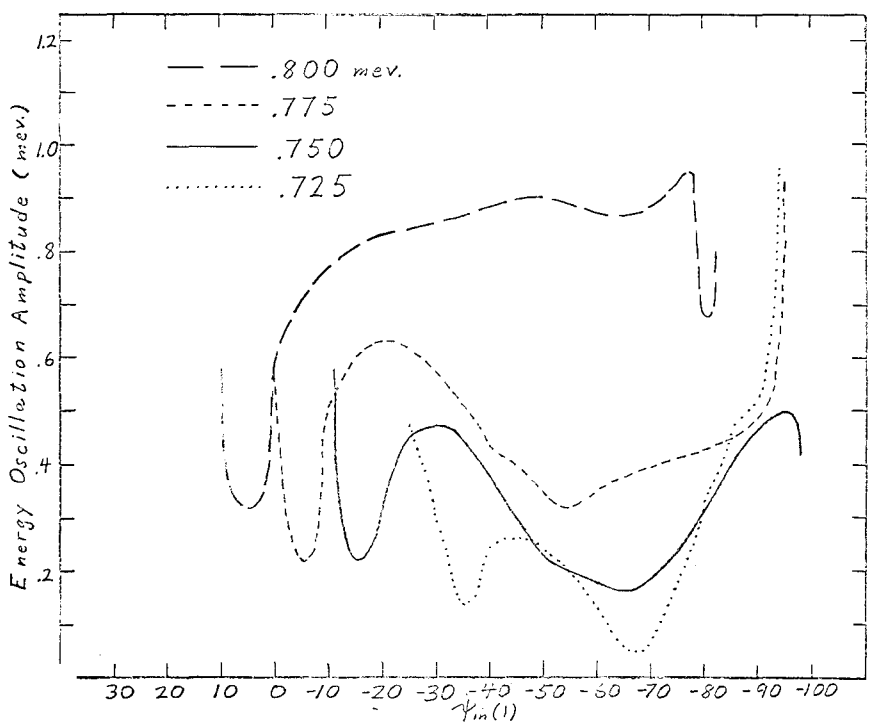

Figure 7: Final energy oscillation amplitude as a function of initial phase, $\psi_{in}(1)$, for various initial energies when the errors of Table II are present.